PERGAMON

International Journal of Heat and Mass Transfer 43 (2000) 3061–3072

International Journal of HEAT and MASS TRANSFER

www.elsevier.com/locate/ijhmt

Thermal analysis of the volume absorber in pulsed excimer laser calorimeters

D.H. Chen, Z.M. Zhang*

Department of Mechanical Engineering, University of Florida, P.O. Box 116300, Gainesville, FL 32611, USA

Received 20 May 1999; received in revised form 8 November 1999

Abstract

Thermal modeling and analysis of the volume absorber in the pulsed excimer laser calorimeters are very important. In this work, Gaussian distributions are used to model the temporal and spatial distributions of the laser beam and an exponential decay function is used to model the internal absorption of the laser power. A finite-element method is employed to simulate the space- and time-dependence of temperature in the volume absorber. A three-dimensional model and an axial-symmetric model are built and used to study the heating effects of single pulse and multiple pulses on the present design, respectively. Furthermore, a new design is proposed, in which the absorber is not optically thick. A one-dimensional model and an axial-symmetric model, in which the reflection at the interface and the absorption on the copper surface are considered, are used to study the heating effects of single pulse and multiple pulses on the new design. The comparison of the present design to the new design shows that the energy loss and nonequivalence in the new design are smaller than those in the present design. Hence, the new design can increase the accuracy and dynamic range of calorimeters. This work will help the future design of optical calorimeters for measuring the pulse energy of excimer lasers in the deep ultraviolet.

1. Introduction

Electrically calibrated laser calorimeters have been developed during the past 30 years at the National Institute of Standards and Technology (NIST) as national reference standards for calibrating laser power and energy meters used in industry and research laboratories [1,2]. Along with the developments of laser applications, C-series, Q-series and K-series calorimeters have been designed and used as standard energy meters for lasers with different modes of operation, powers and wavelength ranges. C-series calorimeters were developed for measuring the continuous wave laser radiation in the power range between 1 mW and 2 W; K-series calorimeters were built for measuring lasers operating at power levels above those applicable to the C-series calorimeters; Q-series calorimeters were fabricated for measuring the pulsed-laser energy, especially that produced by Q-switched Nd:YAG lasers operating at a wavelength of 1.06 μm [1]. Excimer lasers at the wavelength of 248 nm are widely used in semiconductor industries and in advanced materials processing [3–5]. Two calorimeters (QUV-1 and QUV-2) were designed and built for measuring and calibrating the radiant energy of 248 nm excimer laser pulses at NIST [6].

* Corresponding author.
E-mail address: zzhang@cimer.me.ufl.edu (Z.M. Zhang).

0017-9310/00/$ - see front matter
PII: S0017-9310(99)00355-5

Nomenclature

a absorption coefficient, $4\pi\kappa/\lambda$ (cm^{-1})
b $D/2\sqrt{\ln 2}$ (cm)
c constant defined in Eq. (2)
c_p specific heat (J/g K)
D full width at half maximum (FWHM) beam diameter (cm)
h heat transfer coefficient (W/cm^2 K)
k thermal conductivity (W/cm K)
L total thickness of the glass and copper (cm)
L_1 thickness of the glass plate (cm)
m pulse number
N repetition rate (s^{-1})
n refractive index
P average power (W)
Q energy per pulse (J)
q'' heat flux on the copper surface (W/cm^2)
$\dot{q}$ total heat generation rate (W/cm^3)
$\dot{q}_1$ heat generation rate caused by the incident beam (W/cm^3)
$\dot{q}_2$ heat generation rate caused by the reflected beam (W/cm^3)
R reflectance
r distance to the center of the laser beam (cm)
T temperature (K)
T_0 ambient temperature (K)
t time (s)
t_m time at which the pulse power is maximum (s)

Greek symbols
α thermal diffusivity (cm^2/s)
ϵ total emissivity
θ_1 angle of incidence (rad)
θ_2 angle of refraction (rad)
κ extinction coefficient
λ wavelength (μm)
ρ density (g/cm^3)
σ Stefan–Boltzmann constant, 5.67×10^{-12} W/cm^2 K^4
τ $\tau_p/2\sqrt{\ln 2}$ (s)
τ_p FWHM pulse width (s)

Subscripts
a air
c copper
g glass

The trend in microelectronics towards printing features of 0.18 μm and below has motivated the development of photolithographic techniques using argon fluoride (ArF) excimer lasers at the 193 nm wavelength. Indeed, the recent Semiconductor Industry Association roadmap lists 193 nm as one of the options for printing feature of 0.18 μm, along with extensions of 248 nm. The change in wavelength from 248 to 193 nm requires parallel progress in the calibration technologies, optical materials and photoresist chemistries and processes [3]. In order to calibrate the laser power at the wavelength of 193 nm, it is necessary to design and construct an electrically calibrated optical calorimeter that can be used as a standard for absolute laser energy measurements at 193 nm. This will require the selection of a volume absorbing material appropriate for excimer laser at the wavelength of 193 nm and modifications to the existing laser calorimeter designed for the 248 nm excimer laser. Concerns for this approach are possible thermal nonequivalence and radiative heat loss. Presently available commercial devices based on absorbing glasses show significant damage when used with 193 nm excimer lasers.

Based on the work of Leonhardt and Scott [6] of the 248 nm calorimeter, a design was made for the 193 nm calorimeter, as shown in Fig. 1. The calorimeter cavity is made of 0.2 mm thick copper. An electrical heater is attached to the back of the bottom plate to calibrate the calorimeter electrically. Two volume absorbers used to absorb the energy of excimer laser are epoxied to the inside walls of the cavity. They are made of volume absorbing glass plates, whose thicknesses are chosen according to the glass absorption coefficient. Glass plates of low reflectance and extremely low diffuse reflectance are used to achieve nearly 100% absorption inside the cavity. In the present calorimeter design, the copper cavity is suspended to an isothermal heat sink. The temperature difference between the cavity and the heat sink is measured by thermocouples. The measurement principles of laser calorimeters have been described in the literature [2,6].

In order to select the volume absorbing glass appropriate for the excimer laser at the wavelength of 193 nm, thermal modeling and analysis are performed to obtain the temperature distribution of the glass and copper at the bottom of the cavity, during and after the pulse heating. The effects of various pulse parameters on the maximum temperature increase are examined. Although the thermal time constant of the calorimeters is on the order of 10 s, understanding the heat transfer mechanisms in the bottom plate of the cavity during short (nanoseconds) pulse heating is very important for the design and evaluation of 193 nm calorimeters.

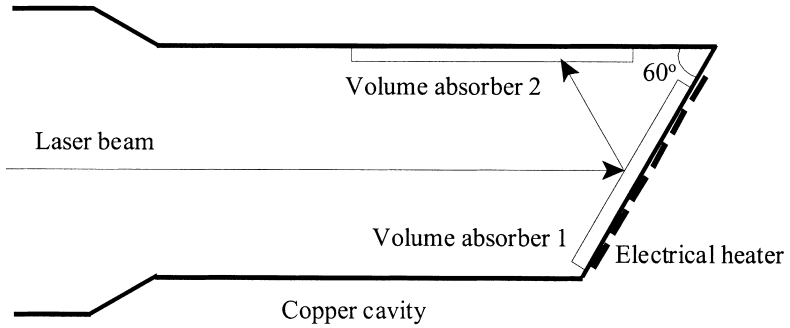

Fig. 1. Schematic of the calorimeter cavity.

2. Thermal model

Heat transfer processes during excimer laser irradiation of materials have been investigated by many researchers. Xu et al. [5,7] performed heat transfer measurements and analysis on the melting of thin polysilicon layers and the plasma induced by laser pulses. In these studies, heat conduction in the solid near the center of the laser beam was assumed to be one-dimensional. Fushinobu et al. [8] investigated the thermal characteristics of polymers irradiated by excimer laser pulses. They assumed that the laser pulse radiation supplies a heat flux at the surface of a semi-infinite solid with adiabatic boundary conditions.

In the present study, the laser power is absorbed inside the volume absorbing glass. The absorbed laser power is regarded as an internal heat source. As shown in Fig. 2, a thermal model is built based on the volume absorbing glass and the copper plate attached to the glass under tilted laser beam incidence. In this model, the front surface of glass and the back surface of copper are subjected to convection and radiation boundary conditions; the side surfaces of the glass and copper are considered isothermal because the pulse heating has very little influence on the temperature field away from the center. Gaussian distributions are used to model the temporal and spatial distributions of the laser power. An exponential decay function is used to model the internal absorption. The effects of the angle of incidence θ_1 and the reflectance at the glass surface R_g are considered. The internal heat generation rate caused by the transmitted laser power is

$$\dot{q}_1(x, y, z, t) = c\mathrm{e}^{-r^2/b^2} e^{-az/\cos\theta_2} \mathrm{e}^{-(t-t_m)^2/\tau^2} \quad (1)$$

In Eq. (1), $a = 4\pi\kappa_g/\lambda$ is the absorption coefficient of the glass at the wavelength of 193 nm, $D = 2b\sqrt{\ln 2}$ is the full width at half maximum (FWHM) beam diam-

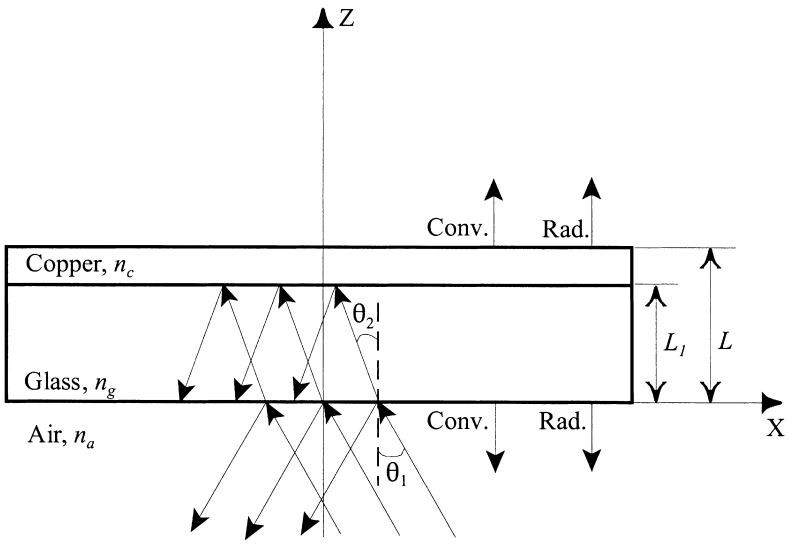

Fig. 2. Illustration of the thermal model, where the side surfaces are assumed isothermal.

eter, $r = ((x + z\tan\theta_2)^2\cos^2\theta_1 + y^2)^{1/2}$ is the distance between the beam line that reaches the point (x, y, z) and the central line of the laser beam in the air, $\theta_2 = \sin^{-1}((n_a/n_g)\sin\theta_1)$ is the angle of refraction, $\tau_p = 2\tau\sqrt{\ln 2}$ is the FWHM pulse width, t_m is the time at which the power is maximum and

$$c = \frac{aQ(1-R_g)\cos\theta_1}{\pi^{3/2}b^2\tau\cos\theta_2} \tag{2}$$

where R_g depends on the refractive index of the glass and the angle of incidence [9] and Q is the energy per pulse. Although the Gaussian distribution extends from $-\infty$ to $+\infty$, it decreases quickly away from the peak. In the present study, the heat generation rate is computed for $r \le 2D$ and from $t_m - 2\tau_p$ to $t_m + 2\tau_p$ and it is set to be zero otherwise.

The energy of laser pulse is absorbed inside the volume absorbing glass. Hence, the transient response of a volume absorbing glass to the incident laser pulse can be described by the three-dimensional heat conduction equation with internal heat generation [10]:

$$\nabla^2 T_g + \frac{\dot{q}(x,y,z,t)}{k_g} = \frac{1}{\alpha_g}\frac{\partial T_g}{\partial t} \tag{3}$$

The transient response of the copper is described by the heat conduction equation without heat generation:

$$\nabla^2 T_c = \frac{1}{\alpha_c}\frac{\partial T_c}{\partial t} \tag{4}$$

The volume absorbing glass is a square plate whose back surface is attached to the copper plate. The front surface of the absorbing glass and the back surface of the copper are subjected to convection and radiation. The initial and boundary conditions on the front surface of the glass and the back surface of the copper are

$$T_g(x,y,z,0) = T_c(x,y,z,0) = T_0 \tag{5}$$

$$k_g\frac{\partial T_g}{\partial z}\bigg|_{z=0} = h_g[T_g(x,y,0,t) - T_0] + \epsilon_g\sigma[T_g^4(x,y,0,t) - T_0^4] \tag{6}$$

$$-k_c\frac{\partial T_c}{\partial z}\bigg|_{z=L} = h_c[T_c(x,y,L,t) - T_0] + \epsilon_c\sigma[T_c^4(x,y,L,t) - T_0^4] \tag{7}$$

Notice that the temperatures at the side surfaces of the glass and copper are set to T_0. The boundary conditions at the interface between the absorbing glass and the copper are

Table 1
Thermophysical properties of the absorbing glass and copper [10–13]

	Glass	Copper
Thermal conductivity, k (W/cm K)	0.0073	4.01
Density, ρ (g/cm^3)	2.3	8.933
Specific heat, c_p (J/g K)	0.7	0.385
Total emissivity, ϵ	0.8	0.03
Refractive index, n	1.5	0.958
Extinction coefficient, κ	9.68×10^{-5}	1.37

$$T_g(x,y,L_1,t) = T_c(x,y,L_1,t) \tag{8}$$

$$k_g\frac{\partial T_g}{\partial z}\bigg|_{z=L_1} = k_c\frac{\partial T_c}{\partial z}\bigg|_{z=L_1} \tag{9}$$

Although the laser pulse is incident at an angle, the temperature distribution of the absorbing glass and copper is symmetric about the x–z plane. Only half of the plate ($y \ge 0$) is studied.

3. Numerical modeling

In the present design, the volume absorber 1 is a square glass plate with a thickness $L_1 = 0.1$ cm and an area 3.2 cm × 3.2 cm. The thickness of the copper cavity is 0.02 cm. The thermophysical properties of the glass and copper are assumed constant in the present study and are listed in Table 1 [10–13].

A commercial finite-element software package, ANSYS 5.4 [14], is employed to model the temperature distribution in the absorbing glass and copper. Solid elements are used to model the glass and copper plates, and surface elements are used to model the free convection and radiation boundary conditions. According to the spatial distribution of the heat generation rate and the numerical test results, the element size in the x–y plane is changed from 0.02 cm close to the center to 0.2 cm near the side boundaries. The mesh scheme in the x–y plane is shown in Fig. 3. Three different sizes are used to mesh the glass in the z direction. The element size is 0.001 cm for $0 \le z \le 0.016$ cm, 0.003 cm for 0.016 cm $\le z \le$ 0.04 cm and 0.015 cm for 0.04 cm $\le z \le$ 0.1 cm. The element size is 0.02 cm in the copper (0.1 cm $\le z \le$ 0.12 cm), i.e. there is only one mesh in the z direction inside the copper. Calculations show that the maximum temperature increases by 1.6% when the smallest element size in the z direction is reduced from 10 to 5 μm. The temperature difference is small enough for the numerical solution to be considered stable, suggesting that the mesh scheme is appropriate.

The initial condition is a uniform temperature $T_0 =$

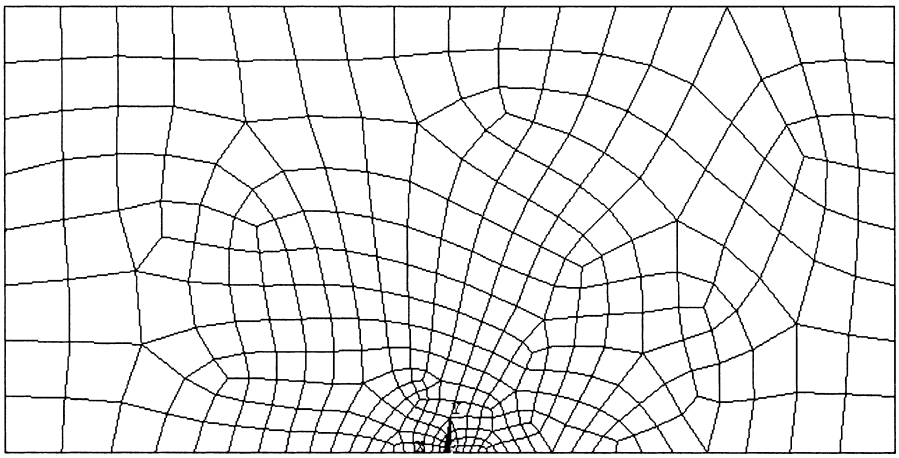

Fig. 3. Mesh scheme on the x–y plane.

300 K inside the glass and copper. The total time required to model one pulse is determined by the inverse of the pulse repetition rate ($1/N$). For each pulse, the heat generation rate is nonzero only at the initial period equal to $4\tau_p$, i.e. the heating process is from $t_m-2\tau_p$ to $t_m+2\tau_p$. For the mth pulse, $t_m=2\tau_p+(m-1)/N$. In the heating process the time step size is taken as $\tau_p/5$. The cooling process (without heat generation) is from $t_m+2\tau_p$ to the beginning of the next pulse, in which the time step size is increased with time from a few nanoseconds to tenths of a second.

When the glass is heated by a single pulse with $\tau_p = 30$ ns, the thermal diffusion length in the $4\tau_p$ heating process can be estimated by $\sqrt{4\tau_p\alpha_g} \approx 0.1$ μm. Hence, heat conduction can be neglected during the heating process. When the surface temperature of the glass is assumed to be 1000 K, the heat loss by free convection is $\approx 10^{-7}$ J/cm^2 and that by radiation is $\approx 10^{-6}$ J/cm^2, which are much less than the laser energy flux at the center of the glass surface. Therefore, the heating process is nearly adiabatic. The adiabatic model is then used to estimate the maximum temperature increase at the end of the heating process. The maximum temperature increase (ΔT_m) is at the center of the glass surface and can be calculated by the following equation:

$$\Delta T_m = \frac{1}{(\rho c_p)_g}\int_{t_m-2\tau_p}^{t_m+2\tau_p} \dot{q}_1(0,0,0,t)\,dt \tag{10}$$

For the absorption coefficient $a = 63\ \text{cm}^{-1}$, pulse width $\tau_p = 30$ ns and pulse energy $Q = 5$ J, the maximum temperature increase at the end of the heating process is 152.8 K calculated from Eq. (10) and 147 K obtained from the numerical simulation. The relative temperature difference is 3.8%. This difference is mainly caused by the element size in the z direction. When the element size in the z direction is reduced, the numerical result becomes closer to the theoretical prediction. For example, when the element size in the z direction is reduced to 0.1 μm, the temperature increase is 151.8 K and the relative temperature difference is only 0.7%. It takes much more computational time and disk space to model such small elements. Because the objective of the present study is to understand the heat transfer process, extremely high accuracy is not needed. When the time steps are varied in the simulation, it has been found that the step size has little influence on the temperature increase at the end of heating process, presumably because the heating generation rate is symmetric about t_m.

4. Results

In the present design, the absorber is a volume absorbing glass [11] with an absorption coefficient $a = 4\pi\kappa/\lambda = 63\ \text{cm}^{-1}$ and thickness of 0.1 cm; therefore, less than 0.2% of the laser energy penetrates through the glass. Consequently, the heat flux of the laser beam on the copper surface contiguous to the glass is so small that the surface heating and reflection by the glass–copper interface can be neglected. The three-dimensional model is used to predict the temperature distributions and histories of the glass and copper heated by a single laser pulse, whose energy is 5 J, FWHM pulse width is 30 ns and FWHM beam diameter is 1.0 cm. Pulse energy of 5 J is close to the practical limit for most applications of 193 nm lasers. The angle of incidence of the laser beam is 30°. In the three-dimensional model, the influence of the incidence angle on the temperature distribution is considered; the ambient temperature and the initial temperature are

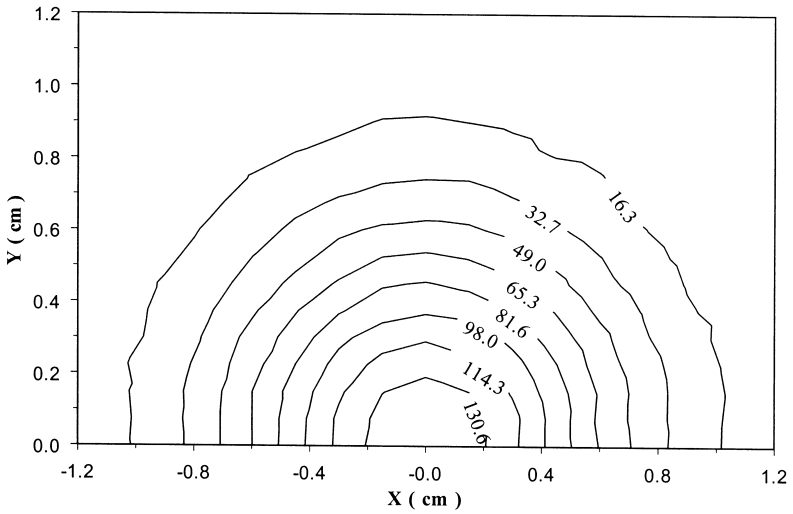

Fig. 4. Temperature contour of the glass surface at the end of the heating process, showing temperature difference $T-T_0$ in K.

300 K. The convection coefficient is assumed to be 0.0008 W/cm^2 K on both sides and the temperature of the isothermal side boundaries is 300 K.

The temperature increases on the glass surface ($z = 0$) at the end of the heating process are shown in Fig. 4. The maximum temperature increase is 147 K at the center of the glass surface. The diameter of the area with temperature increase from 130.6 to 147 K is about 0.4 cm, indicating the central area with high temperature increases is much smaller than the FWHM cross-sectional area of the laser beam. As a result of the oblique incidence, the heat generation rate inside the glass is not symmetric. Influenced by the heat conduction between the surface and the inside, the temperature distribution is not symmetric on the glass surface. When the laser pulse is directly incident on to the surface of copper, the maximum temperature increase is calculated to be 4500 K because of the small radiation penetration depth. The maximum temperature increase for a surface absorbing glass would be 2.2×10^5 K for the same pulse parameters. This indicates that the volume absorbing glass is essential for laser calorimeters with short pulses.

The heat generation rate and the temperature history of the center point of the glass surface in the heating process are shown in Fig. 5. The temperature of the center point on the glass surface increases slowly at the beginning and rapidly as $\dot{q}_1$ increases. After 100 ns, the temperature changes little because the heat generation rate is small and the heat loss increases as the temperature increases. When the energy supplied to the center point by laser heating is less than the energy losses caused by radiation, convection and the inside conduction, the temperature of the center point of the glass surface goes down. This can be seen clearly in Fig. 6, where the temperature histories on the glass surface ($z = 0$) and along the z-axis are shown. In the cooling process the temperatures on the glass surface decrease, but the temperatures inside the glass increase slightly because the heat gained from the glass surface is more than that transferred towards the copper. The maximum temperature increase at the center of the glass–copper interface (0, 0, 0.1) is ≈ 0.13 K, which is very small compared to the 147 K temperature increase at the glass surface. In the cooling process, the temperature difference at locations (0, 0, 0.1) and (0, 0, 0.12) is less than 1 mK because the thermal conductivity of copper is much greater than that of glass. Compared with the temperature difference in the glass, the copper plate can be regarded as an isothermal layer in the heating process of single pulse.

The effects of laser pulse energy, pulse width and beam diameter on the maximum temperature increase have been investigated using the finite element model. The maximum temperature increase is proportional to the pulse energy Q. When the pulse width increases from 10 to 300 ns, the maximum temperature increase decreases by less than 0.02%. The effects of the pulse energy and pulse width on the maximum temperature increase can be understood from the adiabatic model, i.e. Eq. (10). As the beam diameter D increases, the maximum temperature increase decreases by a factor of D^2. This is because $\dot{q}_1$ at $r = 0$ is proportional to the inverse of D^2 (see Eqs. (1) and (2)).

It takes about 5 h to obtain the temperature distribution of glass and copper for one pulse using the three-dimensional model in the 400 MHz personal computer and it takes about 450 Mb disk space to

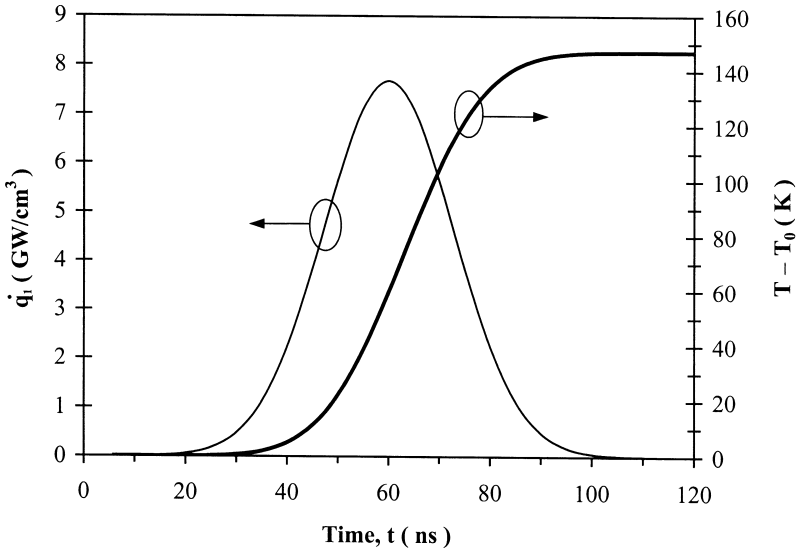

Fig. 5. Heat generation rate and temperature history at the center point of the glass surface in the heating process.

save the database. In order to reduce the computational time and the disk space, an axial-symmetric model is developed to simulate the multiple-pulse heating process. In this model, the glass and copper are treated as circular disks with a radius of 1.6 cm and the laser beam is incident on the glass surface perpendicularly. For comparison, the temperature history is also studied when the glass is heated continuously by the average power using the axial-symmetric model. The average power is calculated by $P = Q \times N$ and the spatial distribution of the heat generation rate is the same as that described in Eq. (1).

Fig. 7 shows the temperature rises at (0, 0, 0) and (0, 0, 0.1) during the first ten pulses with a pulse energy $Q = 5$ J, width $\tau_p = 30$ ns, repetition rate $N = 50\ s^{-1}$ and beam diameter $D = 1.0$ cm, together with those for continuous heating with an average power $P = 250$ W. Notice that the temperature at the back surface of copper (0, 0, 0.12) is very close to that at (0, 0, 0.1). For the pulse heating, the temperature at the

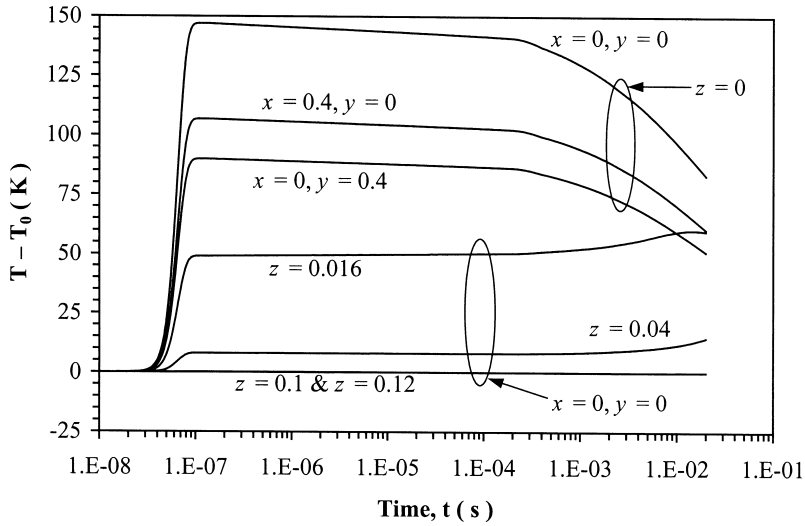

Fig. 6. Temperature histories on the glass surface ($z = 0$) and along the z-axis ($x = 0$, $y = 0$).

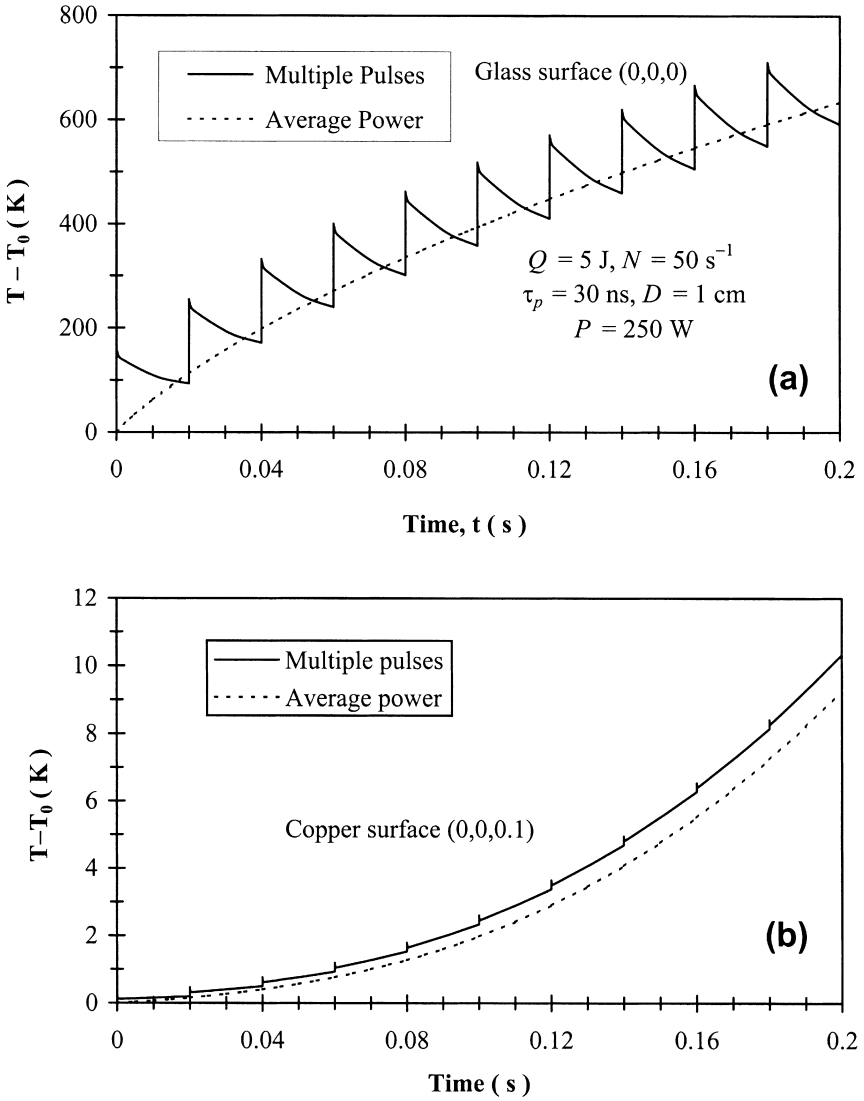

Fig. 7. Comparison of the temperature histories for multiple-pulse heating and average-power heating: (a) glass surface (0, 0, 0); (b) copper surface (0, 0, 0.1).

center of the glass surface goes up quickly in the heating process of each pulse, drops suddenly at the beginning of the cooling process and then goes down slowly until the next pulse. The temperature at (0, 0, 0) goes up gradually for continuous heating. The maximum temperature must not exceed the damage threshold, which limits the number of pulses that can be measured by the calorimeter. Because the peak temperature is higher for the pulse heating than for the average-power heating, the heat loss at the glass surface is greater for pulse heating. This results in a lower temperature for the pulse heating at the end of the cooling process, as shown in Fig. 7(a). As the pulse number increases, the difference in the peak temperature for the pulse heating and the temperature for average-power heating becomes smaller. The heat conduction inside the glass is faster for pulse heating than for continuous heating. As seen from Fig. 7(b), the temperature of the back surface for multiple-pulse heating is higher than that in the average-power heating. Because of the higher peak temperature in the multiple-pulse heating, the energy loss by convection and radiation is more than that in the average-power heating. Hence, the energy stored in the glass and copper in the multiple-pulse heating is smaller than that in the average-power heating.

5. Discussion

For the present design, the thickness of the glass is 6.3 times the radiation penetration depth ($\lambda/4\pi\kappa$). When the laser pulse is incident on the volume absorbing glass, almost all of the transmitted energy of laser pulse is absorbed inside the glass and there is negligible surface heating on the copper surface adjoining the glass. The maximum temperature is on the glass surface and the temperature decreases as z increases. It takes a long time to transfer heat from the glass to copper because of the lower thermal conductivity of glass. As a result, the energy loss is larger for pulse heating than for electrical heating, because in the electrical calibration the highest temperature is located on the back surface of copper where the electrical heater is attached. There may exist a large nonequivalence between laser pulse heating and electrical heating for the present design; this will decrease the accuracy of the laser calorimeter. The high peak temperature on the glass surface may limit the maximum measurable energy, and hence reduce the dynamic range of the calorimeter. In order to increase the accuracy and dynamic range of the calorimeters at the wavelength of 193 nm, a new design is proposed here. As the absorption coefficient of the glass decreases, part of the laser energy will penetrate through the glass and be absorbed directly by the copper surface. Moreover, some of energy will be reflected by the copper surface, resulting in additional heat generation inside the glass. This should help reduce the maximum temperature on the glass surface and heat losses from the glass surface by convection and radiation during laser pulse heating. In the new design, the additional heat generation rate $\dot{q}_2(x, y, z, t)$ caused by the reflected energy from the copper surface can be derived from Eq. (1) by replacing z by $2L_1-z$ and Eq. (2) by the following equation:

$$c = \frac{aQR_c(1-R_g)\cos\theta_1}{\pi^{3/2}b^2\tau\cos\theta_2} \tag{11}$$

The heat flux $q''(x, y, L_1, t)$ on the copper surface is considered. The heat flux absorbed by the copper surface can be obtained from Eq. (1) by setting $z = L_1$ and

$$c = \frac{Q(1-R_g)(1-R_c)\cos\theta_1}{\pi^{3/2}b^2\tau} \tag{12}$$

For the heating time of 120 ns, the thermal diffusive length in the copper is 3.75 μm. Hence, the points beyond 3.75 μm from the center point have little influence on the temperature of the center point. The heat generation rate and heat flux change so little within a few micrometers from the center point that can be considered uniform. Hence, a one-dimensional model is used to study the temperature change near the center of the laser beam, in which the laser beam is incident normal to the glass surface. The heat generation rate and the heat flux on the copper surface in the x–y plane are uniform, equal to the values at the center. The maximum temperature increase on the glass surface and that on the copper surface adjoining the glass are shown in Fig. 8 as functions of the absorption coefficient for $Q = 5$ J and $\tau_p = 30$ ns. As the absorption coefficient decreases, the maximum temperature increase on the copper surface increases due to surface heating, whereas the maximum temperature on the glass surface decreases due to the redistribution of the heat generation rate. When the absorption coefficient becomes smaller than 40 cm^{-1}, the maximum temperature increase on the copper surface is higher than that on the glass surface. Under such conditions, heat is transferred to copper rapidly and the energy loss on the glass surface is small. The nonequivalence between laser pulse heating and electrical heating may be reduced. Therefore, the accuracy and dynamic range of the calorimeter can be improved by selecting an absorbing glass with smaller absorption coefficient or simply reducing the thickness of the glass in the present design.

The temperatures at the centers of the glass surface (0, 0, 0) and the copper surface (0, 0, 0.1) in the heating process are shown in Fig. 9 for $a = 30\ cm^{-1}$. The temperature of the copper surface increases faster than that of the glass surface because of the surface heating effect. Although the maximum temperature increase on the copper surface of 188.5 K is much higher than that on the glass surface, it drops rapidly because the thermal conductivity of copper is much greater than that of glass. The temperature gradient in the z direction after the heating process is much less in this case than in the present design with $a = 63\ cm^{-1}$ (see Fig. 6).

The axial-symmetric model has been extended to study the multiple-pulse heating process for absorption coefficients below 63 cm^{-1}. In this model, the heat flux on the copper surface and the additional heat generation rate caused by reflection from the copper surface are considered. Fig. 10 shows the temperature rises at the center points on the glass surface ($z = 0$) and copper surface ($z = 0.1$) for $a = 30\ cm^{-1}$ during the first five pulses using the same pulse parameters as those for Fig. 7. The results of the axial-symmetric model and the one-dimensional model are almost the same at the beginning. After the heating process of the first pulse however, lateral heat conduction becomes important and the one-dimensional model fails to predict the temperature history at the centerline. In the heating process of each pulse, the temperature at (0, 0, 0.1) increases and decreases suddenly. Due to the heat conduction from the glass to copper, the temperature at (0, 0, 0.1) increases slightly in the cooling process.

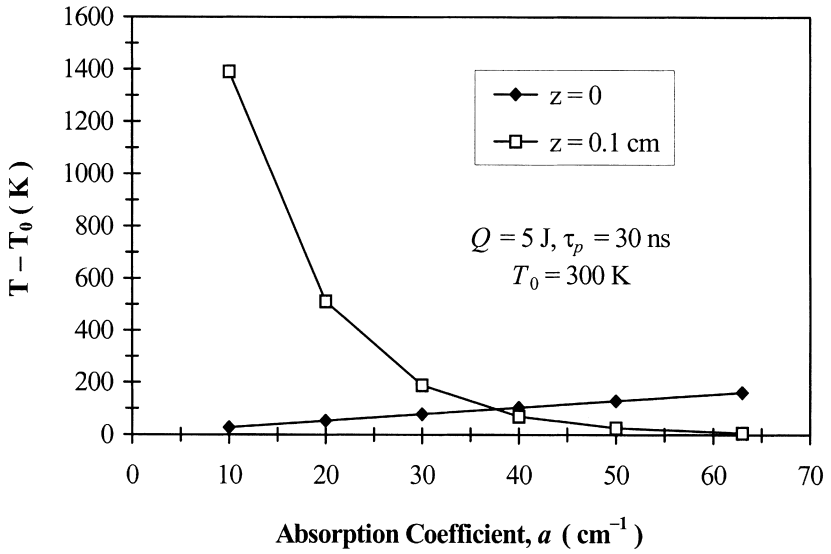

Fig. 8. Comparison of the maximum temperature rise at $z = 0$ (glass surface) to that at $z = 0.1$ cm (copper surface).

Compared to the present design (see Fig. 7), the temperature at the center of the glass surface is much smaller at the end of the heating process of each pulse. For example, at the end of the first pulse and fifth pulse, the temperature rises at (0, 0, 0) are, respectively, 78 and 281 K as shown in Fig. 10, which are much smaller than the corresponding values of 161 and 462 K in Fig. 7(a). Because of the low thermal conductivity of glass, the temperatures on the glass surface do not drop very much in the cooling processes. Consequently, the temperature at (0, 0, 0) keeps rising as the number of pulse increases. The maximum temperature on the glass surface exceeds that on the copper surface (0, 0, 0.1) after four pulses. Hence, the damage threshold of glass limits the number of pulses in the multiple-pulse heating process. Further analysis of the new design is needed so that the optimized absorption coefficient can be determined. The epoxy between glass and copper is not considered in the thermal analysis of the new design; however, the thermally conducting epoxy between glass and copper may act as an energy absorber. The effect of the epoxy layer needs to be further investigated.

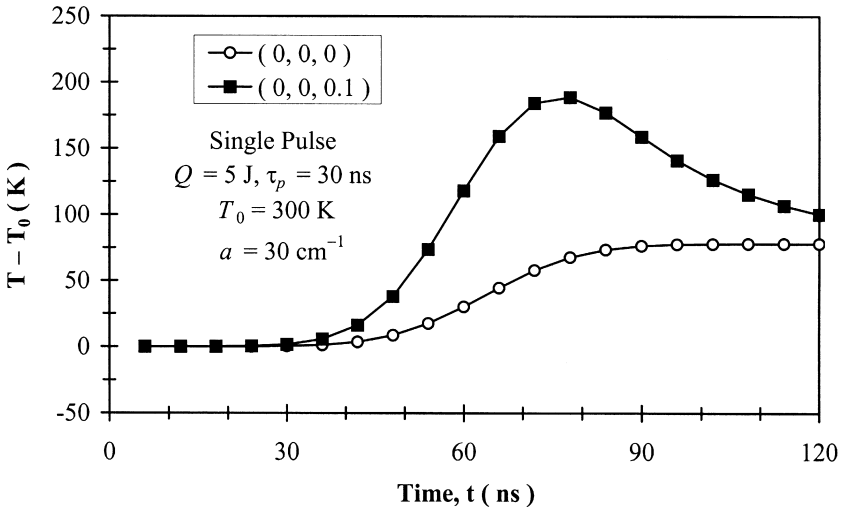

Fig. 9. Comparison of the temperature history at (0, 0, 0) to that at (0, 0, 0.1) in the heating process of one pulse for the new design.

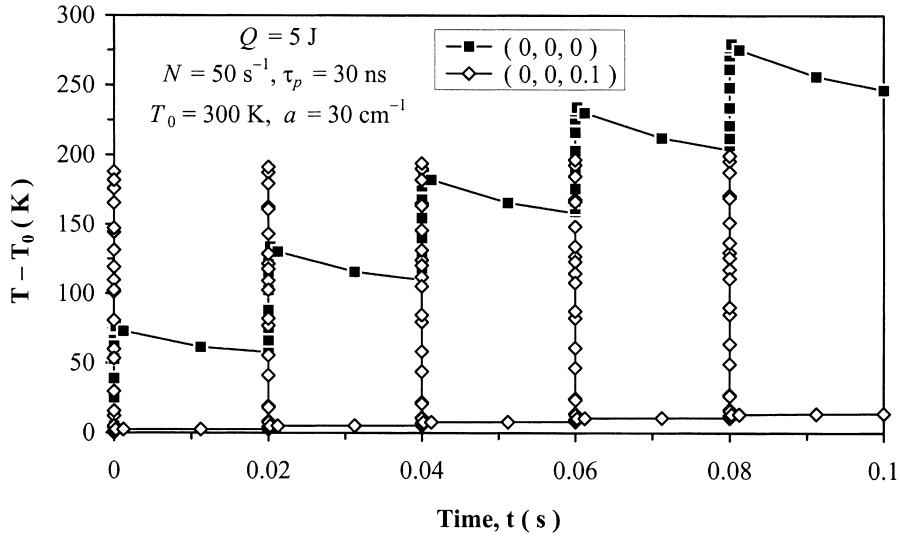

Fig. 10. Comparison of the temperature history at (0, 0, 0) to that at (0, 0, 0.1) in the heating process of multiple pulses for the new design.

6. Conclusions

The present design of a 193 nm pulse laser calorimeter is analyzed by using finite-element models. The heating process for a single pulse is almost adiabatic because the heating time is only 120 ns, but the high temperature on the glass surface and low thermal conductivity of glass cause a large energy loss after the heating process. In the multiple-pulse heating process, temperatures on the glass surface and the copper surface increase with the number of pulses and are higher than those in the average-power heating process. Therefore, the energy stored in glass and copper for multiple-pulse heating is smaller than that for average-power heating. The high peak temperature on the glass surface may limit the number of pulses that can be measured. The large heat loss during the laser pulse heating process may yield a large nonequivalence between laser heating and the electrical calibration.

A new design is presented to reduce the temperature increase on the glass surface and the temperature gradient inside glass, and to accelerate the heat conduction to copper. The maximum temperature increase in the heating process of one pulse moves from the glass surface to the copper surface when the absorption coefficient of glass drops to below 40 cm^{-1}. The large thermal conductivity of copper can reduce the temperature difference in the z direction when the absorption coefficient of glass is below 40 cm^{-1}. For multiple-pulse heating, the peak temperature at the center point of the copper surface increases slowly, and that at the center of the glass surface is significantly reduced compared to the present design. The energy loss and nonequivalence are smaller than those for the present design. Hence, the new design will improve the accuracy and dynamic range of calorimeters. Future research is needed to find a glass material with an absorption coefficient <40 cm^{-1} at the wavelength of 193 nm as well as to evaluate the effect of epoxy absorption. This work is useful for the future design of 193 nm laser calorimeters and, in a broader scope, for the development of standard energy meters for measuring deeper ultraviolet laser pulses.

Acknowledgements

This work has been partially supported by the Optoelectronics Division of the National Institute of Standards and Technology at Boulder, CO. The authors wish to thank Marla Dowell, Rodney Leonhardt, Christopher Cromer and Thomas Scott for valuable information and discussion. Ravi Kumar and Ferdinand Rosa are acknowledged for carefully reviewing the manuscript. Z.M.Z. is grateful to the support of the National Science Foundation through the CAREER Program (CTS-9875441).

References

[1] T.R. Scott, NBS laser power and energy measurements, in: Proceedings SPIE 888, 1988, pp. 48–54.
[2] Z.M. Zhang, D.J. Livigni, R.D. Jones, T.R. Scott, Thermal modeling and analysis of laser calorimeters, Journal of Thermophysics and Heat Transfer 10 (1996) 350–356.

[3] M. Rothschild, A.R. Forte, R.R. Kunz, S.C. Palmateer, J.H.C. Sedlacek, Lithography at a wavelength of 193 nm, IBM Journal of Research and Development 41 (1997) 49–54.
[4] J. Webb, J. Nemechek, Optical fabrication rises to the 193-nm challenge, Laser Focus World (February 1997) 75–82.
[5] X. Xu, C.P. Grigoropoulos, R.E. Russo, Heat transfer in excimer laser melting of thin polysilicon layers, Journal of Heat Transfer 117 (1995) 708–715.
[6] R.W. Leonhardt, T.R. Scott, Deep-UV excimer laser measurements at NIST, Proceedings SPIE 2439 (1995) 448–459.
[7] X. Xu, K.H. Song, Radiation transfer in pulsed-laser-induced plasma, Journal of Heat Transfer 119 (1997) 502–508.
[8] K. Fushinobu, J. Kimizuka, I. Satoh, Y. Kurosaki, Heat transfer characteristics in polymers with excimer laser irradiation, Transport Phenomena in Materials Processing and Manufacturing, ASME-HTD 336 (1996) 39–44.
[9] R. Siegel, J.R. Howell, Thermal Radiation Heat Transfer, 3rd ed., Hemisphere Publishing, Washington, 1992 (ch. 4).
[10] F.P. Incropera, D.P. DeWitt, Fundamentals of Heat and Mass Transfer, 4th ed., Wiley, New York, 1996 (ch. 2 and Appendix A).
[11] Y.S. Touloukian, R.W. Powell, C.Y. Ho, P.G. Klemens, Thermal radiative properties: nonmetallic solids, in: Thermophysical Properties of Matter, vol. 8, IFI/Plenum, New York, 1970, p. 1569.
[12] E.D. Palik, Handbook of Optical Constants of Solids, Academic Press, 1985, pp. 284–285 and 753–763.
[13] Corning Inc., Corporate Headquarters, Corning, NY 14831.
[14] ANSYS Inc., Canonsburg, PA.